Front. Comput. Sci., 2015, 9(5): 678–690
DOI 10.1007/s11704-015-3400-2

RESEARCH ARTICLE

Character recognition based on non-linear multi-projection profiles measure

K C SANTOSH (✉)[1], Laurent WENDLING[2]

1 US National Library of Medicine (NLM), National Institutes of Health (NIH), Bethesda MD 20894, USA
2 SIP-LIPADE, Université Paris Descartes (Paris V), Paris 75270 Cedex 06, France

Abstract In this paper, we study a method for isolated handwritten or hand-printed character recognition using dynamic programming for matching the non-linear multi-projection profiles that are produced from the Radon transform. The idea is to use dynamic time warping (DTW) algorithm to match corresponding pairs of the Radon features for all possible projections. By using DTW, we can avoid compressing feature matrix into a single vector which may miss information. It can handle character images in different shapes and sizes that are usually happened in natural handwriting in addition to difficulties such as multi-class similarities, deformations and possible defects. Besides, a comprehensive study is made by taking a major set of state-of-the-art shape descriptors over several character and numeral datasets from different scripts such as Roman, Devanagari, Oriya, Bangla and Japanese-Katakana including symbol. For all scripts, the method shows a generic behaviour by providing optimal recognition rates but, with high computational cost.

Keywords character recognition, the Radon features, dynamic programming, shape descriptors

1 Introduction

1.1 Context

With the advent of handwriting recognition technology since a few decades [1,2], applications are challenging. For example, handwriting recognition principally entails optical character recognition (OCR) [3–7] is becoming an integral part of document scanners that include applications such as postal processing, script recognition, banking, security (signature verification, for instance) and language identification.

Handwritten character recognition usually means to convert or to translate human writing into the corresponding computer (printed) character. In this domain, the major difficulties in character recognition can be summarised as follows.

- *Structure similarities* between the classes is the primary difficulties; it usually refers to multi-class similarity. It happens more in cursive nature of scripts like Devanagari and Bangla.
- *Deformations* can be from any range of shape variations including geometric transformation such as translation, rotation, scaling and even stretching.
- *Defects* yield imperfections due to printing, optics, scanning, binarisation and poor segmentation.

To cope aforementioned difficulties, in handwriting recognition, besides pre-processing, optimal or accurate feature selection is an important issue [8]. Both structural and statistical features as well as their combination have been widely used [9,10]. Structural features tend to vary since characters' shapes vary widely. As a consequence, local structural properties like intersection of lines, number of holes, concave arcs, end points and junctions change time to time. In those situations, statistical approaches [11] tolerate to a few extent, with no substantial change in the global signatures.

Received October 28, 2013; accepted July 16, 2014

E-mail: santosh. kc@nih. gov

Therefore, the present work is inspired to use statistical feature to represent isolated handwritten characters, numerals as well as symbols. In other words, it is more focussed on shape descriptors and their performances for handwritten character recognition.

Since there exists large variation in shapes and writing styles, OCR systems (for unconstrained scripts in particular) do not provide optimal accuracy. Despite those circumstances, it is desirable to develop shape representation such that it can be used for machine recognition [12–15]. To represent shape of the character, contour-based shape descriptors have been widely used in comparison to region-based ones. Fourier processing of the image is an example of using contour information [16–19]. Besides, curvature approaches [20–22] basically describe shapes in the scale space using the maximum of the curvature feature vector by using boundary contours. The similarity between shapes can be measured by the distance between scale space representations. Further, the shape context (SC) [23,24] is robust to small perturbations while it does not guarantee scale-invariance. On the other side, common methods on region-based shape descriptors are based on moment theory [25] that includes geometric, Legendre, Zernike moments (ZM) [26], as well as pseudo-Zernike moments. Contour-based descriptors on the whole, are appropriate for silhouette shapes since they cannot capture the interior content as well as disconnected shapes or shapes with holes. To represent internal structure of the shape, unlike in Fourier descriptors (FD), Zhang and Lu [27] have proposed a region-based generic Fourier descriptor (GFD) that avoids the problem of rotation in the Fourier spectra. Recently, the use of polar shape descriptors has been mentioned in Ref. [28]. Overall, in almost all global signal-based descriptors [29], to satisfy common geometric invariance properties, the use of normalisation process introduces errors as well as they are sensitive to noise, eventually affecting the whole recognition process.

Before considering shape analysis in character recognition, the following are the worth-considering issues:

- *Plug and play* A single and integrated open source toolset will be a global choice since it can be reused as plug and play [19] as a generic method. In character recognition, not a single OCR engine can handle different scripts – which is in fact necessary to reduce the cost.
- *Non-parametric method* The very common implementation problem is the inability to assume the shape distribution of the patterns in the feature space. Consequently, non-parametric methods are much more practical.

Besides, feature selection must be sufficiently enriched with important information. To represent the pattern, global shape representation is a premier choice due to its simplicity as well as it sometimes does not require extra pre-processing and segmentation process as in local pattern representation. To accomplish recognition, matching is another concern. Feature selection corresponds to the matching techniques. For instance, fixed size pattern representation as in global signal-based shape descriptors [26,27,30], provide immediate matching while dynamic time warping (DTW) for instance, has been popularly used for non-linear sequences having potentially different lengths.

1.2 Outline of the method

In those respects, the paper presents an idea to represent an isolated character via multi-projection profiles with the help of the Radon transform [31] and recognition is made with the help of DTW [32,33]. Thanks to DTW, it avoids compressing pattern representation into a single vector e.g., [30], which may miss important information. The concept of the work is originally derived for off-line signature verification [34,35]. This concept later extended to solve several different pattern recognition problems including character [36,37].

The Radon transform is essentially a set of parametrised histograms or features. Therefore, unlike in previous works [34–37], the method addresses the optimal selection of number of bins rather than using just the straightforward discrete Radon transform. Besides, the paper is the thorough extension of the work [38] where we have attested the possibility of doing character recognition, i.e., the method takes advantages of the Radon transform and DTW, and validates over several different numeral, character and symbol datasets from different scripts such as Roman, Devanagari, Bangla, Oriya and Japanese-Katakana. Our study suggests that the method can be compared with state-of-the-art shape descriptors in terms of recognition rate but on the other hand, it possesses high computational cost.

1.3 Organisation of the paper

The rest of the paper is organised as follows. The proposed method is explained in Section 2, which mainly includes character representation and matching. Section 3 provides a series of tests. It includes a comprehensive study of a set of major state-of-the-art of shape descriptors and thorough analysis with respect to the difficulties associated with sample images. The paper is concluded in Section 4.

2 Method

2.1 Pre-processing

The preliminary task is to do pre-processing since characters tend to be highly degraded as they are taken from newspaper, postal cards etc. under varying different lighting conditions, for instance. It mainly considers stroke synthesis, thresholding, gray-scale to binary conversion; noise removal, foreground textual information extraction by removing background [39]. However, this introduces many ad-hoc techniques. This work does not aim to develop pre-processing technique.

In this work, isolated character images are simply converted to binary. Otsu method has been found to be prominent to handle gray-scale images [40]. However, it does not suit for all types of sample images used in the paper. In such a case, while converting, an average *gray-scale* pixel intensity value (in the range of 70–100) is used to make a threshold that goes differently from one dataset to another. Figure 1 shows a few examples of it. In this illustration, binary conversion is followed by contour detection and thinning using basic image processing tools.

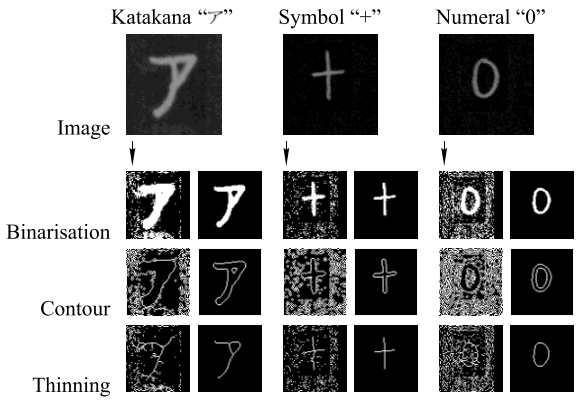

Fig. 1 An example of binarisation. In every sample image, conventional gray-thresholding is shown in the first column while use of average *gray-scale* intensity value is shown in the second column

2.2 Feature selection

2.2.1 The Radon transform

Besides pre-processing, recognition system is based on how characters are represented [8]. In this work, the Radon transform is used to represent patterns [31] to select several different number of projections.

Let $\wp(x, y)$ in $\mathbb{R}^2$ be an original binary pattern, defined in the domain χ:

$$\wp(x,y) = \begin{cases} 1, & \text{if } \wp(x,y) \in \chi, \\ 0, & \text{otherwise.} \end{cases} \tag{1}$$

As shown in Fig. 2, a collection of projections of the pattern at different angles refers to the Radon transform [31]. In other words, the Radon transform for any image pattern $\wp(x, y)$ and for a given set of angles can be thought of as computing the projection of all non-zero points. The resulting projection is the sum of the non-zero points for any pattern $\wp(x, y)$ in each direction, which eventually form a matrix. Therefore the integral of $\wp$ over a line $\mathcal{L}(\rho, \theta)$ in $\mathbb{R}^2$ represented as $\mathcal{L} = \{(x, y) \in \mathbb{R}^2 : x\cos\theta + y\sin\theta = \rho\}$, can formally be expressed as,

$$R(\rho,\theta) = \int_{-\infty}^{\infty}\int_{-\infty}^{\infty} \wp(x,y)\delta(x\cos\theta + y\sin\theta - \rho)\mathrm{d}x\mathrm{d}y, \tag{2}$$

where $\delta(.)$ is the Dirac delta function,

$$\delta(x) = \begin{cases} 1, & \text{if } x = 0, \\ 0, & \text{otherwise.} \end{cases}$$

Also, $\theta \in [0, \pi]$ and $\rho \in [-\infty, \infty]$. For the Radon transform, $\mathcal{L}_i$ be in normal form (ρ_i, θ_i). For all θ_i, the Radon transform now can be described as the length of intersections of all lines $\mathcal{L}_i$. Note that the range of ρ i.e., $-\rho_{\min} < \rho \leqslant \rho_{\max}$ is entirely based on the size of pattern.

2.2.2 Features set

As said before, the Radon transform is essentially a set of parametrised histograms or features since projecting angle extends over $[0, \pi]$. Each bin yields a projection profile i.e., the Radon histogram. As in Fig. 2, we use projection profiles from the Radon transform. In generic form, a complete set of the Radon features $R(\rho, b)$ can be expressed as,

$$\mathcal{F} = \{\mathbf{F}_b\}_{b=1,2,\ldots,B}, \tag{3}$$

where B is the total number of bins and is computed by considering the projection angular step. A single Radon feature at bin b is $\mathbf{F}_b$ is the collection of histograms at every discrete projection angle.

To make the Radon transform invariant to affine transformations, we consider the following properties.

1) Translation We use image centroid (x_c, y_c) such that translation vector is $\vec{u} = (x_c, y_c)$: $R(\rho - x_c\cos\theta - y_c\sin\theta, \theta)$. Therefore, translation of f results in the shift of its transform in ρ by a distance equal to the projection of translation vector of the line $\mathcal{L}$.

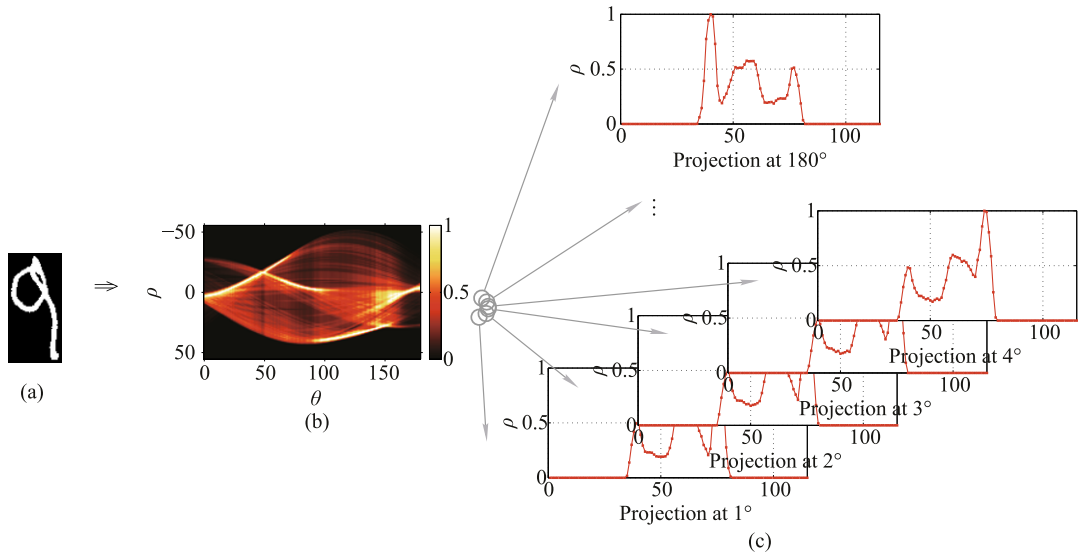

Fig. 2 An illustration of the projection profiles from Radon transform. (a) A sample; (b) the complete Radon transform features; (c) several possible projection profiles over $[0, \pi]$ the Radon histograms or features

2) Scaling Features are normalised into $[0, 1]$ at every projecting angle.
3) Rotation If angle of rotation is α, then $R^{\alpha}(\rho, \theta) = R(\rho, \theta + \alpha)$. This simply implies a circular shift of the features from where it is rotated.

2.3 Feature matching

As explained in Section 2, we have a collection of set of features $\mathcal{F}$ in a specified number of bins B, to represent any pattern $\wp$. Now, a feature at bin b can be represented as,

$$\mathcal{F} = \{f_l\}_{l=1,2,\ldots,L}, \tag{4}$$

where $l \in \rho$.

Given two patterns: query $\wp^q$ and database $\wp^d$, matching can be obtained between corresponding features from $\mathcal{F}^q$ and $\mathcal{F}^d$. The Radon transform generates different ρ sizes depending on the image size. In order to be able to adapt to these differences in size, DTW algorithm is employed. In what follows, matching computation between two features will be explained first and then derived the matching score between the whole patterns.

2.3.1 DTW as a non-linear similarity measure

DTW allows us to find the dissimilarity between two non-linear sequences potentially having different lengths [32,33].

Let us consider two Radon features at bin b, representing

$$\begin{aligned} \mathbf{F}^q &= \{f_k^q\}_{k=1,2,\ldots,K}, \\ \mathbf{F}^d &= \{f_l^d\}_{l=1,2,\ldots,L}, \end{aligned} \tag{5}$$

respectively for $\wp^q$ and $\wp^d$ patterns. At first, a matrix $\mathcal{M}$ of size $K \times L$ is constructed. Then for each element in matrix $\mathcal{M}$, local distance metric $\delta(k, l)$ between the events e_k and e_l is computed, and $\delta(k, l)$ can be expressed as, $\delta(k, l) = (e_k - e_l)^2$, where $e_k = f_k^q$ and $e_l = f_l^d$. Let $D(k, l)$ be the global distance up to (k, l),

$$D(k, l) = \min \begin{bmatrix} D(k-1, l-1), \\ D(k-1, l), \\ D(k, l-1) \end{bmatrix} + \delta(k, l), \tag{6}$$

with an initial condition $D(1, 1) = \delta(1, 1)$ such that it allows warping path going diagonally from starting node $(1, 1)$ to end (K, L). The main aim is to find the path for which the least cost is associated. The warping path therefore provides the difference cost between the compared sequences. Formally, the warping path is,

$$\mathcal{W} = \{w_t\}_{t=1,2,\ldots,T}, \tag{7}$$

where $\max(k, l) \leqslant T < k + l - 1$ and tth element of $\mathcal{W}$ is $w(k, l)_t \in [1 : K] \times [1 : L]$ for $t \in [1 : T]$. The optimised warping path $\mathcal{W}$ satisfies the following three conditions.

a) Boundary condition: $w_1 = (1, 1)$ and $w_T = (K, L)$,
b) Monotonicity condition: $k_1 \leqslant k_2 \leqslant \cdots \leqslant k_K$ and $l_1 \leqslant l_2 \leqslant \cdots \leqslant l_L$,
c) Continuity condition: $w_{t+1} - w_t \in \{(1, 1)(0, 1), (1, 0)\}$ for $t \in [1 : T - 1]$.

a) conveys that the path starts from $(1, 1)$ to (K, L), aligning all elements to each other. b) forces the path advances one step at a time. c) restricts allowable steps in the warping path to adjacent cells, never be back. Note that c) implies b).

We then define the global distance between $\mathbf{F}_k^q$ and $\mathbf{F}_l^d$ as,

$$\Delta(\mathbf{F}^q, \mathbf{F}^d) = \frac{D(K, L)}{T}. \quad (8)$$

The last element of the $K \times L$ matrix, normalised by the T provides the DTW-distance between two sequences where T is the number of discrete warping steps along the diagonal DTW-matrix.

Until now, we provide a global concept of using DTW distance for non-linear sequence alignment. In order to provide faster matching, we have used local constraint on time warping proposed in [41]. We have $w(k, l)_t$ such that $l-r \leqslant k \leqslant l+r$ where r is a term defining a reach i.e., allowed range of warping for a given event in a sequence. With r, upper and lower bounding measures can be expressed as,

$$\begin{aligned} \text{Upperbound}U_k &= \max(f^q_{k-r} : f^q_{k+r}), \\ \text{Lowerbound}L_k &= \min(f^q_{k-r} : f^q_{k+r}). \end{aligned} \quad (9)$$

Therefore, for all k, an obvious property of U and L is $U_k \geqslant f^q_k \geqslant L_k$. With this, we can define a lower bounding measure for DTW:

$$\text{LB\_Keogh}(\mathbf{F}^q, \mathbf{F}^d) = \sqrt{\sum_{k=1}^{K} \begin{cases} (f^d_k - U_k)^2, & \text{if } f^d_k > U_k; \\ (f^d_k - L_k)^2, & \text{if } f^d_k < L_k; \\ 0, & \text{otherwise.} \end{cases}} \quad (10)$$

Since this provides a quick introduction of local constraint for lower bounding measure, we refer to Ref. [41] for more detail.

2.3.2 Matching score and time complexity

Aggregating distances between the radon features in all corresponding bins $b \in B$ between $\wp^q$ and $\wp^d$ yields a global pattern matching score,

$$\text{Dist.}(\wp^q, \wp^d) = \sum_{b \in B} \Delta(\mathbf{F}^q_b, \mathbf{F}^d_b). \quad (11)$$

Overall, the Radon feature alignment goes one-to-one basis since we assume that test images are not rotated and thus B is the maximum possible number of matchings, i.e., time complexity can be expressed as $O(B)$. The overall execution time however, depends on how many bins are taken. Its value determines the number of matchings associated with it. As a consequence, it advances linearly with the number of patterns in the database.

2.3.3 Illustration

Figure 3 shows the matching score matrix for a few sample images from a particular known class of Devanagari numeral "**0**" with different shapes and sizes. This illustration aims to demonstrate how far DTW absorbs the varying the Radon features (i.e., histograms) sizes resulting from image signal variations due to different sizes. To compute distance between them, the discretised Radon transform is used. In this illustration, the small difference in matching score between the two samples is mostly due to shape variation. Further, it is important to notice that the method performs well for possible shape variations due to deformations and distortions in addition to the size difference. Therefore, it is well-suited for natural handwriting (Section 1).

2.4 Character recognition

The Dist.(,) of course, conveys how similar/dissimilar a database character is with respect to a query. In order for similarity to be ranging from 0 to 1, for any query q, we normalise $\text{Dist.}(\wp^q, \wp^d), d \in \{1, 2, \ldots, DB\}$ with

$$\overline{\text{Dist.}}(,) = \frac{\text{Dist.}(,) - \text{Dist.}^{\min}\cdot(,)}{\text{Dist.}^{\max}\cdot(,) - \text{Dist.}^{\min}\cdot(,)}.$$

We then express similarity between the two characters,

$$\text{Similarity}(\wp^q, \wp^d) = 1 - \overline{\text{Dist.}}(\wp^q, \wp^d). \quad (12)$$

For recognition, the closest candidate from the database character having the highest similarity with respect to query, is said to be the recognised character, i.e., $\underset{d \in 1,2,\ldots,DB}{\text{argmax}} \{\text{Similarty}(\wp^q, \wp^d)\}$.

3 Experiments

3.1 Datasets

Several different datasets from different scripts including symbol[2)] are tested in order to provide a wide range of natural writing styles. They are grouped into three categories.

1) Numeral datasets: Roman, Devanagari, Oriya and Bangla [42,43],
2) character datasets: Roman, Japanese-Katakana and Bangla, and
3) symbol dataset.

Figure 4 shows a sample for each class for all categories. Numeral category consists of ten classes for all scripts. In case of character datasets, number of classes vary from one script to another: 26 classes for Roman, 47 classes for

[2)] ISI character datasets for Indian scripts, CVPR unit, India. ETL3 and ETL5 datasets for Roman and Japanese-Katakana scripts, AIST, Japan

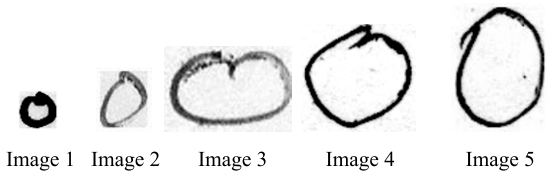

(a)

	Image 1	Image 2	Image 3	Image 4	Image 5
Image 1	0.00	2.00	5.00	7.00	8.00
Image 2		0.00	5.00	6.00	7.00
Image 3			0.00	5.00	6.00
Image 4				0.00	3.00
Image 5					0.00

(b)

Fig. 3 Matching scores between sample images (same class) from Devanagari numeral dataset. Matching score matrix shows the behaviour of the method when shape and size vary. (a) Sample images with shape and size variation; (b) matching score @ 10^{-2}

Fig. 4 Sample images from several different scripts for both numeral and character categories including symbol dataset. (a) Numeral; (b) character; (c) symbol

Japanese-Katakana and 50 classes for Bangla. Symbol category consists of 11 classes.

3.2 State-of-the-art shape descriptors

As said in Section 1, to validate the method, a comprehensive study is made by taking a set of major global signal-based shape descriptors as benchmarking methods such as:

1) $\mathcal{R}-$signature [30],
2) GFD [27],
3) SC [23],
4) ZM 26.

For those descriptors, it is important to fit the best parameters. For $\mathcal{R}-$signature, the discrete Radon transform is used, i.e., range of projecting angle is $[0, \pi]$ by default. In case of GFD, the parameters are tuned as, radial (4:12) and angular (6:20) frequencies to get the best combinations with the provided range. For SC, the test follows [23], i.e., 100 number of sample points are used. In case of ZM, 36 *zernike* functions of order less than or equal to seven has been used.

In the proposed method, a series of tests will be made for all possible projection angle–range (Section 2) over $[0, \pi]$ so that different number of bins are selected starting from the 180 to two Radon features. To simplify, we will call it as $\mathcal{D}-$Radon. Since the proposed method and $\mathcal{R}-$signature are basically based on the Radon transform theory to represent patterns, let us keep on eyes to realise how it has been advanced i.e., the recognition performance gap that can exist between them.

3.3 Evaluation protocol

While experimenting, every test sample is matched with training candidates and the closest one is reported. As described in Section 4, the closest candidate corresponds to the labelled class, which we call "character recognition". Formally, recognition rate can be defined as

$$\text{recognitionrate} = \frac{c}{Q}, \tag{13}$$

where c is the number of correctly recognised candidates and Q is the total number of test candidates.

To evaluate the performance of the methods, $\mathcal{K}-$fold cross validation (CV) has been implemented unlike traditional dichotomous classification. In $\mathcal{K}-$fold CV, the original sample for every class is randomly partitioned into $\mathcal{K}$ sub-samples. Of the $\mathcal{K}$ sub-samples, a single sub-sample is used for validation, and the remaining $\mathcal{K}-1$ sub-samples are used for training. This process is then repeated for $\mathcal{K}$ folds, with each of the $\mathcal{K}$ sub-samples used exactly once. Finally, a single value results from averaging all. The opposite process holds for inverse $\mathcal{K}-$fold CV, i.e., $\mathcal{K}-1$ sub-samples are used for testing.

While experimenting, tests move from normal $\mathcal{K}-$fold CV to inverse. This means that every test goes from $\mathcal{K}-1$ to $\mathcal{K}-4$ training sub-samples when $\mathcal{K}=5$. The aim of the use of such a series of rigorous tests is to avoid the biasing of the samples that can be possible in conventional dichotomous dataset classification.

3.4 Results and analysis

3.4.1 Results outline

In this section, we aim to discuss about how results will be presented.

Table 1 shows the average recognition rates for all datasets (category-wise) using $\mathcal{K}-$fold CV, where one can notice the following.

1) In all categories, comparison is first made among the benchmarking methods (from the state-of-the-art shape descriptors) before confronted "the best" performer with $\mathcal{D}-$Radon for several different number of bins. To make easy comparison, the compared results are highlighted.
2) For benchmarking methods, the best performer is highlighted first. Then in case of the proposed method, the highlighted numeric figures from different number of bins will then be identified as optimal selection of B when also considering computational complexity.
3) The bold-faced numeric figure is the best score from both worlds.

Further, in order to attest the significance of the performance differences between $\mathcal{D}-$Radon at every separate and benchmarking methods, we have provided their probability (p) score using 2-tailed t-test, assuming the null hypothesis in Table 2 where the level of required significance is 0.05. We note the following:

1) if $p = 0.05$, the null hypothesis were correct (i.e., the methods do not differ);
2) if $p < 0.05$, the methods are said to be statistically significant;
3) if $p < 0.001$, the methods are statistically highly significant.

Having this idea, in Table 2, we will have an opportunity to realise the statistical performance differences made by $\mathcal{D}-$Radon over every benchmarking method. These differences are highlighted at every pre-defined value of B.

On the whole, we are not limited just on the straightforward recognition rates and their comparison but also pro-

viding the statistical significance of their performance differences.

3.4.2 Results

Based on the framework presented in the earlier section, dataset category-wise results (reported in Tables 1 and 2) will be discussed.

• Numeral datasets

In Roman dataset, all shape descriptors provide encouraging recognition performances, having almost similar results (Table 1). The significant differences between them exist in case of Devanagari and Bangla datasets (Table 2). SC yields consistent recognition rates for all while others do not follow such a characteristic. GFD however, comes closer to SC. $\mathcal{D}$−Radon is now confronted with SC and sometimes with GFD. In this category, there exists no surprising differences between them, i.e., a marginal difference of 1%–2%. However, we note that the number of bins $B = 90$ for $\mathcal{D}$−Radon, provides better results and $B = 60$ can also be compared with.

While keeping a closer look at Table 2, $\mathcal{D}$−Radon provides that the differences are statistically significant with

- $\mathcal{R}$−signature upto $B = 36, 9, 9$, and 18 respectively for Roman, Oriya, Devanagari and Bangla datasets;
- ZM upto $B = 2$ for all datasets except Roman, i.e., $B = 36$;
- GFD upto $B = 60$ for all datasets except Oriya, i.e., $B = 90$;
- SC at $B = 180$ for all datasets except Bangla where no decision can be made.

Table 1 Average recognition rate in % using $\mathcal{K}$−fold cross validation ($\mathcal{K} = 5$)

			Benchmarking methods				$\mathcal{D}$−Radon for different values of B						
Dataset		Training	$\mathcal{R}$−sign.	ZM	GFD	SC	180	90	60	36	18	09	02
	Roman	$\mathcal{K}-1$	78	83	97	98	**100**	**100**	**100**	88	79	76	71
		$\mathcal{K}-2$	75	78	95	97	**100**	**100**	99	84	75	74	68
		$\mathcal{K}-3$	70	74	94	96	**98**	96	95	79	74	71	66
		$\mathcal{K}-4$	66	67	91	96	**98**	96	94	77	74	68	67
	Oriya	$\mathcal{K}-1$	58	44	98	98	**100**	98	92	81	67	60	51
		$\mathcal{K}-4$	52	38	96	96	**98**	97	94	77	64	55	48
		$\mathcal{K}-3$	46	43	85	93	**98**	96	88	74	62	50	47
Numeral		$\mathcal{K}-4$	43	32	72	92	**97**	92	90	71	68	49	45
datasets	Devanagari	$\mathcal{K}-1$	55	40	86	96	**99**	97	89	79	71	62	52
		$\mathcal{K}-2$	54	40	84	94	**98**	96	87	75	68	59	48
		$\mathcal{K}-3$	50	38	81	93	**98**	94	84	74	66	58	47
		$\mathcal{K}-4$	46	34	69	87	**96**	**95**	83	73	65	55	46
	Bangla	$\mathcal{K}-1$	48	47	73	**95**	**95**	**95**	84	72	60	51	41
		$\mathcal{K}-2$	48	44	69	**94**	**94**	92	79	68	55	48	38
		$\mathcal{K}-3$	46	43	68	91	**93**	86	76	61	54	47	37
		$\mathcal{K}-4$	44	40	64	89	**92**	81	75	59	53	45	36
	Roman	$\mathcal{K}-1$	80	77	96	99	**100**	**100**	**100**	88	83	80	71
		$\mathcal{K}-2$	77	74	94	98	**99**	**99**	96	86	81	79	70
		$\mathcal{K}-3$	75	67	93	97	**98**	97	94	85	77	75	67
		$\mathcal{K}-4$	69	58	91	**98**	**98**	96	93	83	77	74	68
	Katakana	$\mathcal{K}-1$	69	42	88	91	**99**	97	88	82	77	71	62
Character		$\mathcal{K}-2$	66	37	85	87	**97**	96	86	80	75	66	62
datasets		$\mathcal{K}-3$	63	34	84	84	**96**	94	85	77	75	66	60
		$\mathcal{K}-4$	59	28	78	81	**96**	93	84	76	72	64	60
	Bangla	$\mathcal{K}-1$	22	11	23	55	**77**	73	69	58	55	45	33
		$\mathcal{K}-2$	18	09	22	49	**74**	71	66	58	54	43	29
		$\mathcal{K}-3$	14	06	18	46	**72**	70	65	57	51	42	27
		$\mathcal{K}-4$	11	06	16	43	**71**	70	63	55	50	39	25
	Symbol	$\mathcal{K}-1$	81	82	85	90	**100**	**100**	99	91	82	80	76
Symbol		$\mathcal{K}-2$	78	77	82	88	**100**	**100**	98	89	81	78	74
dataset		$\mathcal{K}-3$	74	73	75	82	**100**	99	97	85	78	77	73
		$\mathcal{K}-4$	70	69	72	76	**100**	99	97	85	78	76	72

Table 2 Probability value (p) using t-test, considering 5−fold cross validation

Dataset		Benchmarking methods	$\mathcal{D}$−Radon for different values of B						
			180	90	60	36	18	09	02
Numeral datasets	Roman	$\mathcal{R}$sign.	**0.001 0**	**0.000 6**	**0.000 3**	**0.000 2**	0.168 2	1.000 0	0.109 7
		ZM	**0.003 9**	**0.002 7**	**0.001 8**	**0.012 0**	1.000 0	0.143 8	0.065 0
		GFD	**0.011 4**	**0.015 3**	**0.022 1**	0.002 9	0.000 1	0.000 0	0.000 0
		SC	**0.002 8**	0.194 1	0.824 0	0.005 2	0.000 0	0.000 3	0.000 0
	Oriya	$\mathcal{R}$−sign.	**0.000 2**	**0.000 0**	**0.000 2**	**0.000 0**	**0.013 1**	**0.006 0**	0.4918
		ZM	**0.000 1**	**0.000 0**	**0.000 4**	**0.000 3**	**0.005 5**	**0.009 9**	**0.021 9**
		GFD	**0.023 1**	**0.044 0**	0.579 7	0.059 1	0.040 3	0.003 2	0.003 8
		SC	**0.027 2**	0.252 2	0.035 7	0.000 1	0.000 5	0.000 0	0.000 0
	Devanagari	$\mathcal{R}$−sign.	**0.000 0**	**0.000 1**	**0.000 2**	**0.000 3**	**0.000 5**	**0.003 4**	0.091 7
		ZM	**0.000 0**	**0.000 0**	**0.000 0**	**0.000 0**	**0.000 0**	**0.000 0**	**0.002 1**
		GFD	**0.015 5**	**0.021 7**	0.127 6	0.206 2	0.021 2	0.003 4	0.001 7
		SC	**0.028 1**	0.172 7	0.007 2	0.000 6	0.000 1	0.000 0	0.000 0
	Bangla	$\mathcal{R}$−sign.	**0.000 0**	**0.000 1**	**0.000 3**	**0.003 4**	**0.003 6**	0.141 1	0.000 9
		ZM	**0.000 0**	**0.000 1**	**0.000 0**	**0.001 1**	**0.000 2**	**0.000 4**	**0.001 6**
		GFD	**0.000 2**	**0.000 7**	**0.000 8**	0.101 8	0.000 3	0.000 0	0.000 0
		SC	0.194 1	0.121 5	0.000 7	0.000 5	0.000 0	0.000 0	0.000 0
Character datasets	Roman	$\mathcal{R}$−sign.	**0.001 2**	**0.000 6**	**0.000 4**	**0.004 3**	**0.048 1**	0.235 1	0.040 1
		ZM	**0.004 3**	**0.003 2**	**0.002 8**	**0.014 4**	**0.038 1**	0.067 8	1.000 0
		GFD	**0.003 6**	**0.000 5**	**0.037 3**	0.000 0	0.000 2	0.000 1	0.000 0
		SC	**0.051 6**	1.000	0.169 6	0.000 7	0.000 5	0.000 4	0.000 0
	Katakana	$\mathcal{R}$−sign.	**0.000 2**	**0.000 1**	**0.000 5**	**0.000 4**	**0.003 0**	0.095 7	0.143 8
		ZM	**0.000 1**	**0.000 0**	**0.000 1**	**0.000 1**	**0.000 2**	**0.000 3**	**0.001 8**
		GFD	**0.003 6**	**0.003 3**	0.236 1	0.018 9	0.003 6	0.000 5	0.000 9
		SC	**0.004 8**	**0.005 1**	1.000 0	0.003 3	0.002 9	0.000 2	0.000 6
	Bangla	$\mathcal{R}$−sign.	**0.000 0**	**0.000 0**	**0.000 0**	**0.000 1**	**0.000 1**	**0.000 2**	**0.000 4**
		ZM	**0.000 0**	**0.000 0**	**0.000 0**	**0.000 0**	**0.000 0**	**0.000 0**	**0.000 0**
		GFD	**0.000 0**	**0.000 0**	**0.000 0**	**0.000 0**	**0.000 0**	**0.000 0**	**0.000 8**
		SC	**0.000 2**	**0.001 2**	**0.000 1**	**0.022 5**	0.065 2	0.023 9	0.000 1
Symbol dataset	Symbol	$\mathcal{R}$−sign.	**0.002 0**	**0.001 5**	**0.001 5**	**0.021 7**	0.072 7	0.295 2	0.235 2
		ZM	**0.002 9**	**0.002 4**	**0.002 3**	**0.003 3**	0.092 9	0.287 1	0.495 0
		GFD	**0.005 6**	**0.004 6**	**0.004 8**	**0.010 7**	0.579 0	0.756 9	0.121 0
		SC	**0.014 8**	**0.012 8**	**0.015 3**	0.161 5	0.155 3	0.079 6	0.023 3

• Character datasets

In Table 1, surprisingly, $\mathcal{R}$−signature provides higher recognition rates in Roman dataset compared to itself in the previous Numeral category. SC, GFD and ZM show similar behaviour as before. The similar characteristics occur in Japanese-Katakana dataset. But in case of Bangla, GFD, ZM and $\mathcal{R}$−signature do not hold the same. Overall, SC provides better recognition performance. In contrast to $\mathcal{D}$−Radon, SC is lagging by approximately 1%, 5% and 22% respectively in Roman, Japanese-Katakana and Bangla datasets. As before, 60 number of bins can be taken for comparison for Roman and Japanese-Katakana datasets while 18, for Bangla dataset.

In Table 2, $\mathcal{D}$−Radon provides that the differences are statistically significant with

- $\mathcal{R}$−signature upto $B = 18, 18$ and 2 respectively for Roman, Japanese-Katakana and Bangla datasets;
- ZM upto $B = 18, 2$ and 2 for Roman dataset and $B = 2$ for both Japanese-Katakana and Bangla datasets;
- GFD upto $B = 60, 90$ and 2 respectively for Roman, Katakana and Bangla datasets;
- SC at $B = 180, 90$ and 36 respectively for Roman, Japanese-Katakana and Bangla datasets.

• Symbol dataset

In this test, $\mathcal{R}$−signature comes closer to all shape descriptors unlike before (Table 1). As in previous experiments, SC provides higher recognition rate. Compared to $\mathcal{D}$−radon, it is less than by more than 10%. Overall, $\mathcal{D}$−Radon yields 100% recognition rate for $B = 180$ and $B = 90$. It is important to notice that 36 number of bins is sufficient to make comparison with SC.

In Table 2, $\mathcal{D}$−Radon provides that the differences are statistically significant with

- $\mathcal{R}-$signature, ZM and GFD upto $B = 36$;
- SC upto $B = 60$.

In all datasets, $\mathcal{D}-$Radon supersedes all methods, while providing small differences with SC, "the best" performer from state-of-the-art of shape descriptors. The notable difference is found to be exist in case of Bangla character and symbol datasets. GFD is following behind the first two. ZM provides substantial difference in recognition rate against GFD, SC and $\mathcal{D}-$Radon. While, $\mathcal{R}-$signature performs far behind all with the difference fairly in large amount.

Another remarkable point is that $\mathcal{D}-$Radon provides competitive recognition rates even when the decrement of number of bins upto 60. 36 number of bins can also comparatively be treated with the state-of-the-art of shape descriptors in a few datasets such as Roman and Symbol. Furthermore, recognition rates ranging from normal $\mathcal{K}-$fold CV to inverse, do not provide a big difference. This means that the method is found to be almost stable even when number of training samples is reduced significantly. To see the stability over the range of $\mathcal{K}-$fold CV to inverse, let us have a look into $\mathcal{D}-$Radon where $B = 180$ (and sometimes 90), there exists very small difference between them, for all tests except for only Bangla character dataset.

3.4.3 Analysis

Considering the datasets (Section 1) used, methods (Section 2) are analysed in response to the evaluation protocol (Section 3) based on experimental results in Table 1 (Section 4). While analysing, recognition performance is taken into account that consists of two major issues:

1) How accurate the system is?
2) How long it takes to process it?

In what follows, both are discussed.

• Accuracy

The accuracy of the recognition engine reflects the discrimination power of the shape descriptor as well as the number of training samples used. Within this framework, a few common difficulties will be discussed. As mentioned in the very beginning of Section 1, let us highlight a few major challenges such as

1) multi-class similarity;
2) symmetric shape similarity;
3) missing parts;
4) stroke length or size variation.

Multi-class similarity is one of the major problems in character recognition as shown in Fig. 5. It happens more in Bangla character dataset. In such a dataset, the recognition rate determines the actual discrimination power difference that exists between the shape descriptors since one cannot judge the superiority by taking a simple dataset like Roman. In addition, shape descriptors with rotation invariant properties have been affected from those samples as shown in Fig. 5 (b). This means that symmetric shape similarity due to rotation, translation and even scaling affects the recognition engine. Such samples are found in Japanese-Katakana character dataset, Oriya and Devanagari numeral dataset as well as symbol dataset. In symbol dataset, symmetric shape similarity severely affects the existing shape descriptors even though sample images are quite simple. Similarly, missing parts introduce shape similarity. Besides, sample images with long ascender and/or descender part of the stroke affects SC compared to GFD. Due to these circumstances, existing methods require more training samples in order to get varieties of writing in the labelled known classes. This has been attested in experimental results (Table 1) where substantial decrement in recognition rate has been observed when training samples are reduced from $\mathcal{K} - 1$ to $\mathcal{K} - 4$, where $\mathcal{K} = 5$. Despite, $\mathcal{D}-$Radon provides fairly better in those situations. Furthermore, size variation does not have significant affect as it employs DTW for radon features alignment.

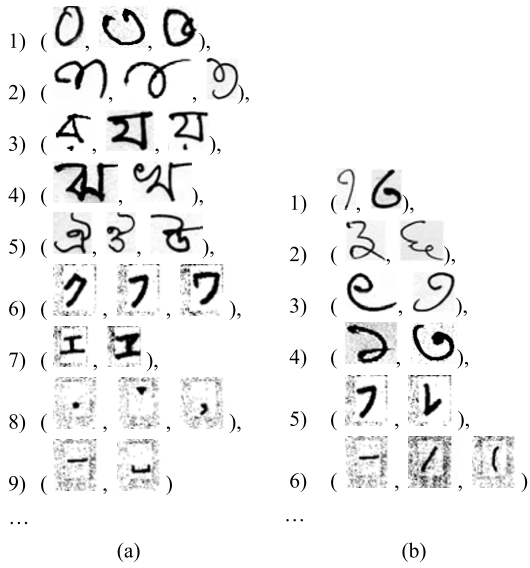

Fig. 5 Difficulties in character recognition — a few examples. (a) Multi–class similarity; (b) symmetric shapes

• Computational cost

Another important issue is computational cost. In $\mathcal{D}-$Radon, running time complexity is high since it uses classical DTW for matching. As far as concern to computational cost, the observed average running time for feature selection and matching for a single pair, for all methods is provided in

Table 3. All tests have been made using MATLAB 7.8.0 in Linux platform. In $\mathcal{D}$−Radon, running time is largely depend on how big the image is and the number of bins used to represent it. An optimal selection of number of bins would be the premier choice to reduce the delay.

Table 3 Average running time/s

Method	Time
1) $\mathcal{R}$-signature [30]	01
2) ZM [26]	04
3) GFD [27]	03
4) Shape Context [23]	16
5) $\mathcal{D}$−Radon	36

On the whole, $\mathcal{D}$−Radon provides optimal recognition performance for all datasets except Bangla character dataset. However, in Bangla character dataset, it provides huge difference with SC — "the best" performer from state-of-the-art so that it makes easier to convey its discriminant power. But on the other hand, its recognition performance does not compete with related OCR engines because they are script dependent. But the method is still competitive by providing its robustness to deformations, shape and size variations including possible defects. To attest it, another relevant experimental test is reported in the following.

3.5 Extensions

The previously used datasets do not really provide a complete framework where the method can show its robustness on different sizes in addition to deformed and distorted models. Therefore, a new Devanagari numeral dataset has been created as shown in Fig. 6, where for each sample, there are five different scaled images (random scaling) and five different deformed and distorted images by just randomly taking out/keeping in black pixels from/in the images.

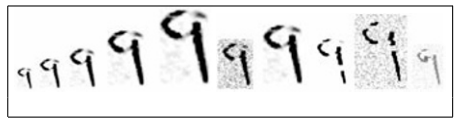

Fig. 6 An example of the new dataset for a single Devanagari numeral sample. It illustrates scaling and deformation plus distortion. The first five samples are scaled images and remaining five are deformed and distorted sample images

As before, all shape descriptors are tested using $\mathcal{K}$−fold CV and average recognition rates are provided in Table 4 and the differences between the methods (in terms of probability value by using t-test) are provided in Table 5.

Table 4 Average recognition rate in % using $\mathcal{K}$−fold cross validation ($\mathcal{K}$ = 5)

		Benchmarking methods				$\mathcal{D}$−Radon for different values of B						
Numeral dataset	Training	$\mathcal{R}$−sign.	ZM	GFD	SC	180	90	60	36	18	09	02
Devanagari	$\mathcal{K}-1$	52	46	81	69	**97**	96	91	84	74	66	56
	$\mathcal{K}-2$	49	45	79	68	**95**	94	88	81	72	65	52
	$\mathcal{K}-3$	48	42	77	66	**94**	92	86	78	69	64	50
	$\mathcal{K}-4$	46	39	74	64	**93**	**92**	86	77	68	62	48

Table 5 Probability value (p) using t-test, considering 5−fold cross validation

	Benchmarking	$\mathcal{D}$−Radon for different values of B						
Numeral dataset	methods	180	90	60	36	18	09	02
Devanagari	$\mathcal{R}$−sign.	**0.000 0**	**0.000 0**	**0.000 0**	**0.000 0**	**0.000 0**	**0.000 0**	**0.010 4**
	ZM	**0.000 0**	**0.000 0**	**0.000 0**	**0.000 0**	**0.000 0**	**0.000 0**	**0.000 2**
	GFD	**0.000 1**	**0.000 2**	**0.000 7**	**0.018 7**	0.000 4	0.000 2	0.000 0
	SC	**0.000 0**	**0.000 0**	**0.000 0**	**0.000 2**	**0.002 2**	0.000 3	0.000 2

Unlike in previous tests, GFD shows better results among the state-of-the-art. In contrast, $\mathcal{D}$−Radon provides significant difference with it. Depending on the pattern complexity, state-of-the-art of shape descriptors' performances vary: sometimes SC (Table 1) and sometimes GFD (Table 4). This means that one cannot receive the consistent recognition performance from the existing shape descriptors. The huge difference that exists with SC between Table 1 and Table 4 is due to two different major factors, i.e., it is not

1) scale invariant;
2) robust to deformations and distortions.

The later factor affects all shape descriptors. For both, $\mathcal{D}$−Radon performs better and provides huge difference with the existing ones. In Table 5, $\mathcal{D}$−Radon provides that the differences are statistically significant with

1) $\mathcal{R}$−signature, ZM upto B = 02;
2) GFD, upto B = 36;
3) SC upto B = 18.

4 Conclusion and future perspectives

In this paper, we have studied a method for character recognition based on the combination of the Radon features i.e., multi-projection profiles for representing the pattern and dynamic programming for non-linear profiles similarity matching. We have found that it can be compared with the state-of-the-art of shape descriptors for isolated off-line character recognition that are taken several different publicly available datasets. Besides, the trade-off between the selection of number of bins or profiles and running time has been clearly shown, but it has not been proved yet.

The method can generally be applied — it provides higher recognition rates for all scripts — since not a single OCR engine can do it. Computing the Radon transform is very simple and immediate. But the execution time for matching is high when using the standard DTW algorithm. Therefore, our further work will be summarised in the following:

1) finding the dynamic trade-off between the number of bins and the execution time and tune the parameters accordingly;
2) reducing the execution time either by applying the advanced DTW or simply using graphical processing units (GPU) and similarly, parallel computing;
3) establishing comparison with the OCR engines of all corresponding scripts.

Along with this, further test on several different publicly available datasets such as NIST, is still our concern.

Acknowledgements Most of the experiments of this paper were done when K C Santosh was with INRIA Nancy Grand Est and Université de Lorraine - LORIA (UMR 7503) research centre France (from 2008 to 2013).

References

1. Plamondon R, Srihari S N. On-line and off-line handwriting recognition: a comprehensive survey. IEEE Transactions on Pattern Analysis and Machine Intelligence, 2000, 22: 63–84
2. Arica N, Yarman-Vural F. An overview of character recognition focused on off-line handwriting. IEEE Transactions on Systems, Man, and Cybernetics, Part C: Applications and Reviews, 2001, 31(2): 216–233
3. Suen C Y, Berthod M, Mori S. Automatic recognition of handprinted characters — the state of the art. Proceedings of the IEEE, 1980, 68(4): 469–487
4. Schantz H F. The History of OCR. Manchester Center, VT: Recognition Technologies Users Association, 1982
5. Davis R H, Lyall J. Recognition of handwritten characters — a review. Image and Vision Computing, 1986, 4: 208–218
6. Govindan V, Shivaprasad A. Character recognition — a review. Pattern Recognition, 1990, 23(7): 671–683
7. Dai R, Liu C, Xiao B. Chinese character recognition: history, status and prospects. Frontiers of Computer Science, 2007, 1(2): 126–136
8. Trier D, Jain A K, Taxt T. Feature extraction methods for character recognition — a survey. Pattern Recognition, 1996, 29(4): 641–662
9. Heutte L, Paquet T, Moreau J V, Lecourtier Y, Olivier C. A structural/statistical feature based vector for handwritten character recognition. Pattern Recognition Letters, 1998, 19(7): 629–641
10. Foggia P, Sansone C, Tortorella F, Vento M. Combining statistical and structural approaches for handwritten character description. Image and Vision Computing, 1999, 17(9): 701–711
11. Jain A K, Duin R P W, Mao J. Statistical pattern recognition: a review. IEEE Transactions on Pattern Analysis and Machine Intelligence, 2000, 22(1): 4–37
12. Shinghal R, Suen C. A method for selecting constrained hand-printed character shapes for machine recognition. IEEE Transactions on Pattern Analysis and Machine Intelligence, 1982, 4(1): 74–78
13. Mantas J, Heaton A. Handwritten character recognition by parallel labelling and shape analysis. Pattern Recognition Letters, 1983, 1: 465–468
14. Campos T E, Babu B R, Varma M. Character recognition in natural images. In: Proceedings of the International Conference on Computer Vision Theory and Applications. 2009, 273–280
15. Mahmoud S A. Arabic character recognition using fourier descriptors and character contour encoding. Pattern Recognition, 1994, 27(6): 815–824
16. Granlund G H. Fourier preprocessing for hand print character recognition. IEEE Transactions on Computers, 1972, C–21(2): 195–201
17. Lai M T, Suen C Y. Automatic recognition of characters by fourier descriptors and boundary line encodings. Pattern Recognition, 1981, 14(1-6): 383–393
18. Rauber T, Steiger Garcao A. Shape description by unl fourier features-an application to handwritten character recognition. In: Proceedings of the 11th IAPR International Conference on Pattern Recognition Methodology and Systems. 1992, II:466–469
19. Hopkins J, Andersen T L. A fourier-descriptor-based character recognition engine implemented under the gamera open-source document-processing framework. In: Proceedings of the International Conference on Document Recognition and Retrieval Conference. 2005, 111–118
20. Bernier T, Landry J A. A new method for representing and matching shapes of natural objects. Pattern Recognition, 2003, 36(8): 1711–1723
21. Kopf S, Haenselmann T, Effelsberg W. Enhancing curvature scale space features for robust shape classification. In: Proceedings of the IEEE International Conference on Multimedia and Expo. 2005, 478–481
22. Khoddami M, Behrad A. Farsi and latin script identification using curvature scale space features. In: Proceedings of the Symposium on Neural Network Applications in Electrical Engineering. 2010, 213–217
23. Belongie S, Malik J, Puzicha J. Shape matching and object recognition using shape contexts. IEEE Transactions on Pattern Analysis and Machine Intelligence, 2002, 24(4): 509–522
24. Tepper M, Acevedo D, Goussies N A, Jacobo J C, Mejail M. A decision step for shape context matching. In: Proceedings of the IEEE International Conference on Image Processing. 2009, 409–412
25. Flusser J. On the independence of rotation moment invariants. Pattern Recognition, 2000, 33(9): 1405–1410

26. Kim W Y, Kim Y S. A region-based shape descriptor using zernike moments. Signal Processing: Image Communication, 2000, 16(1-2): 95–102
27. Zhang D, Lu G. Shape-based image retrieval using generic fourier descriptor. Signal Processing: Image Communication, 2002, 17: 825–848
28. Frejlichowski D. Analysis of four polar shape descriptors properties in an exemplary application. In: Proceedings of the International conference on Computer Vision and graphics. 2010, 376–383
29. Zhang D, Lu G. Review of shape representation and description techniques. Pattern Recognition, 2004, 37(1): 1–19
30. Tabbone S, Wendling L, Salmon J P. A new shape descriptor defined on the radon transform. Computer Vision and Image Understanding, 2006, 102(1): 42–51
31. Deans S R. Applications of the Radon Transform. New York: Wiley Interscience Publications, 1983
32. Kruskall J B, Liberman M. The symmetric time warping algorithm: From continuous to discrete. In: Proceedings of Time Warps, String Edits and Macromolecules: the Theory and Practice of String Comparison. 1983, 125–161
33. Keogh E J, Pazzani M J. Scaling up dynamic time warping to massive dataset. In: Proceedings of the European Conference on Principles and Practice of Knowledge Discovery in Databases. 1999, 1–11
34. Coetzer J. Off-line Signature Verification. Dissertation for PhD Degree, University of Stellenbosch, 2005
35. Jayadevan R, Kolhe S R, Patil P M. Dynamic time warping based static hand printed signature verification. Pattern Recognition Research, 2009, 4(1): 52–65
36. Santosh K C, Lamiroy B, Wendling L. DTW for matching radon features: a pattern recognition and retrieval method. In: Proceedings of International Conference on Advances Concepts for Intelligent Vision Systems. 2011, 249–260
37. Santosh K C. Character recognition based on DTW-radon. In: Proceedings of International Conference on Document Analysis and Recognition. 2011, 264–268
38. Santosh K C, Lamiroy B, Wendling L. DTW–radon-based shape descriptor for pattern recognition. International Journal of Pattern Recognition and Artificial Intelligence, 2013, 27(03): 1350008
39. Alginahi Y. Preprocessing techniques in character recognition. Character Recognition, 2010,1–20
40. Otsu N. A threshold selection method from gray-level histograms. IEEE Transactions on Systems, Man, and Cybernetics, 1979, 9(1): 62–66
41. Keogh E J. Exact indexing of dynamic time warping. In: Proceedings of the 28th International Conference on Very Large Data Bases. 2002, 406–417
42. Bhowmik T K, Parui S K, Bhattacharya U, Shaw B. An HMM based recognition scheme for handwritten oriya numerals. In: Proceedings of the International Conference on Information Technology. 2006, 105–110
43. Bhattacharya U, Chaudhuri B B. Handwritten numeral databases of indian scripts and multistage recognition of mixed numerals. IEEE Transactions on Pattern Analysis and Machine Intelligence, 2009, 31(3): 444–457

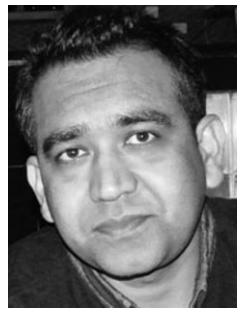

K C Santosh is currently a research fellow at the US National Library of Medicine (NLM), National Institutes of Health (NIH), USA. Before this, K C worked as a postdoctoral research scientist at the Université de Lorraine – LORIA (UMR-7503) Campus Scientifique and ITESOFT, France. He earned his PhD in Computer Science from INRIA Nancy Grand Est, Université de Lorraine, France in 2011, MS in information technology by research and thesis from the school of ICT, SIIT, Thammasat University, Thailand in 2007, and BS in electronics and communication from PU, Nepal, in 2003. His research interests include document image analysis, document information content exploitation, biometrics (such as face) and (bio)medical image analysis.

Laurent Wendling received the PhD in computer science from the University of Paul Sabatier, Toulouse, France in 1997. He received the HDR degree in 2006. From 1993 to 1999, he was with the IRIT in the field of pattern recognition. From 1999 to 2009, he was an assistant professor at the ESIAL Nancy, and a member of LORIA in the field of symbol recognition. His current research topics are spatial relation, feature selection, and image segmentation. He is currently a full professor at the Paris Descartes University, in the field of computer science. He is also the group leader of the SIP team, LIPADE.